Subscriber access provided by UNIV OF CINCINNATI

Research Article

Properties of a Stilbene-Containing Gemini Photosurfactant: Light-Triggered Changes in Surface Tension and Aggregation

Julian Eastoe, Margarita Sanchez Dominguez, Paul Wyatt, Andrew Beeby, and Richard K. Heenan

Langmuir, **2002**, 18 (21), 7837-7844• DOI: 10.1021/la0257384 • Publication Date (Web): 26 June 2002

Downloaded from http://pubs.acs.org on March 9, 2009

More About This Article

Additional resources and features associated with this article are available within the HTML version:

- Supporting Information
- Links to the 8 articles that cite this article, as of the time of this article download
- Access to high resolution figures
- Links to articles and content related to this article
- Copyright permission to reproduce figures and/or text from this article

View the Full Text HTML

ACS Publications
High quality. High impact.

Langmuir is published by the American Chemical Society. 1155 Sixteenth Street N.W., Washington, DC 20036

Properties of a Stilbene-Containing Gemini Photosurfactant: Light-Triggered Changes in Surface Tension and Aggregation

Julian Eastoe,*,† Margarita Sanchez Dominguez, and Paul Wyatt*,‡

School of Chemistry, University of Bristol, Bristol, BS8 1TS United Kingdom

Andrew Beeby

Department of Chemistry, University of Durham, South Road, Durham, DH1 3LE United Kingdom

Richard K. Heenan

ISIS-CLRC, Rutherford Appleton Laboratory, Chilton, OXON, OX11 0QX United Kingdom

Received March 15, 2002. In Final Form: April 19, 2002

A new photosurfactant has been synthesized, and its photoreactions in water, interfacial properties, and changes in aggregation have been characterized. The compound is a stilbene-containing gemini photosurfactant (SGP), which is of interest because the headgroup spacer is a stilbene chromophore, and it may be prepared initially in the *trans* (*E*-SGP) form. Molecular simulations show that UV-induced reactions cause significant changes in molecular conformation and especially the relative orientation of hydrophobic chains. ^{1}H nuclear magnetic resonance, UV−vis absorption, and liquid chromatography−mass spectroscopy results are consistent with photodimerization in aqueous solutions. Irradiation causes significant changes in surface tension (maximum $\Delta\gamma = -12$ mN m^{-1}) and wettability ($\Delta\theta = -15°$ on hydrophobic glass). Furthermore, small-angle neutron scattering shows the initial *E*-SGP form is present as large vesicle-like aggregates whereas the UV-induced dimer gives small 20 Å spherical charged micelles. These results demonstrate the importance of molecular design for generating effective and efficient photosurfactants.

Introduction

The application and development of photosurfactants is an appealing and maturing field of colloid science. A principal driving force behind surfactant adsorption and aggregation is the "solvophobic effect"; hence, in aqueous systems, control over aggregation and adsorption states can only be achieved by shifting the balance of hydrophobic and hydrophilic interactions. Typically, this is done by adding electrolyte (ionic amphiphiles), switching pH (zwitterionics), and/or changing the temperature (non-ionics). Alternatively, if surfactants contain a suitable chromophore, then UV−vis light can be used as an external trigger, eliminating the need for composition or temperature changes. Typical photosurfactants contain an isomerisable group, such as azobenzene or stilbene, in the hydrophobic chain[1−16] or a photocleavable headgroup.[17−22] The majority of studies have been with azo-containing surfactants, which undergo isomerization (e.g., refs 4−6) and/or photolysis.[20,21] With compounds of this type, dramatic changes in surface tension ($\Delta\gamma$), up to 40 mN m^{-1}, were reported.[20,21] Photoisomerization of a single chain cationic surfactant was shown to induce a maximum $\Delta\gamma$ of around 13 mN m^{-1} (Du Nouy ring).[6] In the present paper, drop volume tensiometry (DVT) was used, which allows equilibrium γ values to be obtained. Mixtures, such as a specialized cationic bolaform (two-headed) photosurfactant with sodium dodecyl sulfate (SDS), have also

* To whom correspondence should be addressed.

† Tel.: UK + 117 9289180. Fax: UK + 117 9250612. E-mail: julian.eastoe@bristol.ac.uk.

‡ Tel.: UK + 117 9289183. Fax: UK + 117 9298611. E-mail: paul.wyatt@bris.ac.uk.

(1) Kunitake, T.; Nakashima, N.; Shimomura, M.; Okahata, Y. *J. Am. Chem. Soc.* **1980**, *102*, 6642.

(2) Kunitake, T.; Okahata, Y.; Shimomura, M.; Yasunami, S. I.; Takarabe, K. *J. Am. Chem. Soc.* **1981**, *103*, 5401.

(3) Wolff, T.; Klaussner, B.; von Bünau, G. *Prog. Colloid Polym. Sci.* **1990**, *83*, 176.

(4) Hayashita, T.; Kurosawa, T.; Miyata, T.; Tanaka, K.; Igawa, M. *Colloid Polym. Sci.* **1994**, *272*, 1611.

(5) Yang, L.; Takisawa, N.; Hayashita, T.; Shirahama, K. *J. Phys. Chem.* **1995**, *99*, 8799.

(6) Kang, H. C.; Lee, B. M.; Yoon, J.; Yoon, M. *J. Colloid Interface Sci.* **2000**, *231*, 255.

(7) Holmberg, K. *Novel Surfactants*; Surfactant Science Series Vol. 74; Marcel Dekker: 1998; Chapter 11.

(8) Shin, J. Y.; Abbott, N. L. *Langmuir* **1999**, *15*, 4404.

(9) Karthaus, O.; Shimomura, M.; Hioki, M.; Tahara, R.; Nakamura, H. *J. Am. Chem. Soc.* **1996**, *118*, 9174.

(10) Sakai, H.; Matsumura, A.; Yokoyama, S.; Saji, T.; Abe, M. *J. Phys. Chem. B* **1999**, *103*, 10737.

(11) Song, X.; Perlstein, J.; Whitten, D. G. *J. Am. Chem. Soc.* **1997**, *119*, 9144.

(12) Kim, I.; Rabolt, J. F.; Stroeve, P. *Colloid Surf., A* **2000**, *171*, 167.

(13) Mooney, W. F.; Brown, P. E.; Russel, J. C.; Costa, S. B.; Pedersen, L. G.; Whitten, D. G. *J. Am. Chem. Soc.* **1984**, *106*, 5659.

(14) Holden, D. A.; Ringsdorf, H.; Deblauwe, V.; Smets, G. *J. Phys. Chem.* **1984**, *88*, 716.

(15) Evans, S. D.; Johnson, S. R.; Ringsdorf, H.; Williams, L. M.; Wolf, H. *Langmuir* **1998**, *14*, 6436.

(16) Gustina, D.; Markava, I.; Muzikante, I.; Stiller, B.; Brehmer, L. *Adv. Mater. Opt. Electron.* **1999**, *9*, 245.

(17) Haubs, M.; Ringsdorf, H. *New J. Chem.* **1987**, *11*, 151.

(18) Haubs, M.; Ringsdorf, H. *Angew. Chem., Int. Ed. Engl.* **1985**, *24*, 882.

(19) Arndt, T.; Haüssling, L.; Ringsdorf, H.; Wegner, G. *Adv. Mater.* **1991**, *3*, 58.

(20) Dunkin, I. R.; Gittinger, A.; Sherrington, D. C.; Wittaker, P. *J. Chem. Soc., Chem. Commun.* **1994**, 2245.

(21) Dunkin, I. R.; Gittinger, A.; Sherrington, D. C.; Wittaker, P. *J. Chem. Soc., Perkin Trans 2* **1996**, 1837.

(22) Nukyen, O.; Meindl, K.; Wokaun, A.; Mezger, T. *J. Macromol. Sci., Pure Appl. Chem.* **1995**, *A32* (Suppl. 4), 447.

10.1021/la0257384 CCC: $22.00 © 2002 American Chemical Society
Published on Web 06/26/2002

Scheme 1. Synthesis of *E*-SGP Surfactant

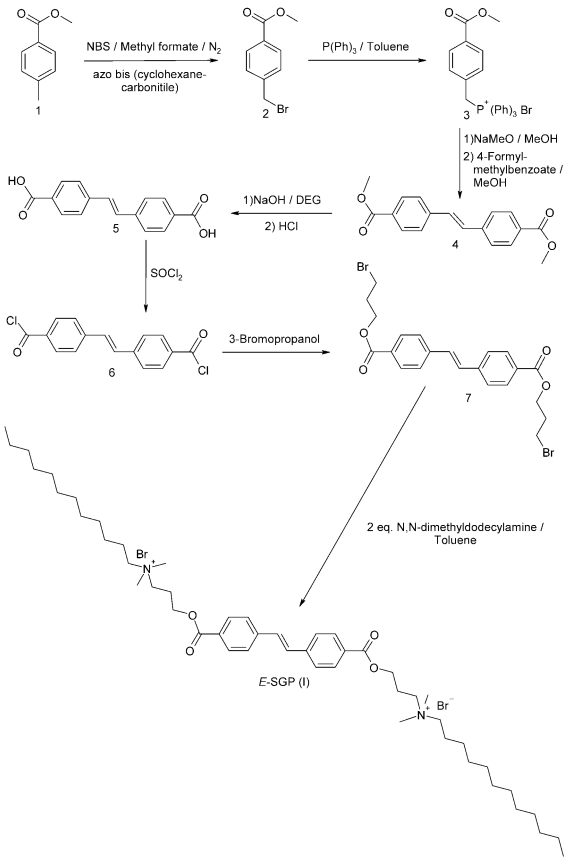

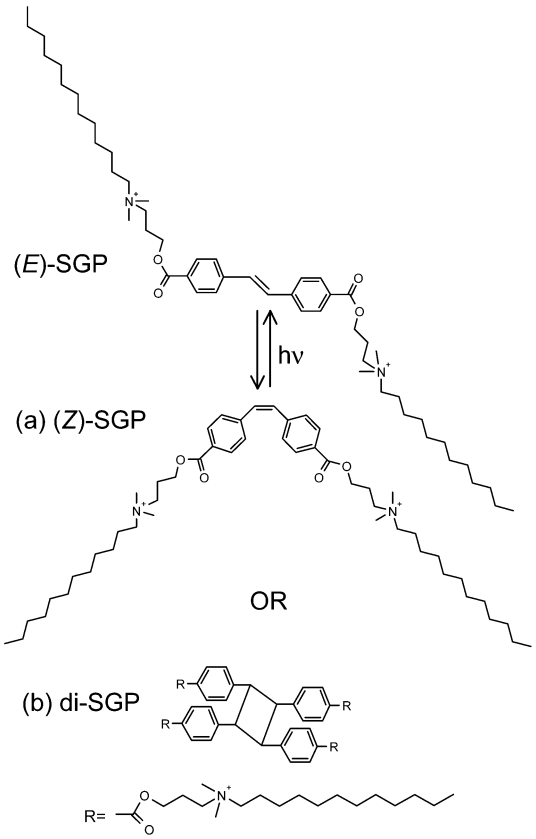

Figure 1. Possible photoreactions of *E*-SGP surfactant: (a) *cis*−*trans* isomerization and (b) dimerization.

been employed.[8] For this combination, dynamic surface tension (DST) can be reduced by as much as 20 mN m^{-1} after illumination.[8] Interestingly, only modest changes in surface tension were obtained with the bolaform alone in the absence of SDS.[8] There are several reports of photoinduced changes in monolayers and Langmuir−Blodget films.[9,12−19] In terms of isomerization, significant effects were observed with water insoluble gemini bearing a stilbene spacer group: a decrease in the surface area per molecule and an increase in collapse pressure was observed on formation of the *cis* isomer.[9] Fluorescence microscopy on this system indicated a photoinduced solid-to-liquid transition in the monolayer. References 8 and 9 indicate that sophisticated molecular structures, such as bolaform or gemini compounds, give rise to enhanced photoinduced interfacial effects. Light-induced changes in aggregation have also been reported.[1,10,11] Kunitake et al. used transmission electron microscopy (TEM) and small-angle light scattering to study changes in aggregation with a single chain azobenzene surfactant.[1] A transition from globular aggregates (200 Å diameter) to short rods (50−70 Å diameter) was observed after irradiation. Dynamic light scattering has also been employed to investigate aggregation of photosurfactants.[11]

On the basis of this literature, it is clear that "smart" molecular design is key for targeting efficient photosurfactants. For example, a gemini surfactant bearing a photoactive group in the spacer would be expected to undergo significant changes in conformation and hence physicochemical properties. With this in mind, a new stilbene-containing gemini photosurfactant (SGP, Scheme 1 and Figure 1) was synthesized. Here, it is demonstrated that the surfactant undergoes photodimerization, and consequently, γ at the air−solution surface decreases up to 12 mN m^{-1} after irradiation. In addition, the contact angles of aqueous solutions on hydrophobically modified glass (octadecyltrichlorosilane, OTS) were decreased by ∼15° after irradiation. There are several disadvantages of using light scattering and TEM for such dilute self-assembly systems, whereas small-angle neutron scattering (SANS) represents an ideal method. SANS experiments with SGP described here demonstrate a dramatic change in aggregate shape and size after irradiation. It would appear that this represents the first use of SANS for investigating photosurfactant micelles. These results confirm the photoactivity of SGP, at the air−water and solid−liquid interfaces as well as in the bulk.

Experimental Section

Scheme 1 represents the synthetic route to the surfactant, and Appendix 1 contains experimental details.

Techniques. Glassware cleaning, drop volume measurements (Lauda TVT1), and conductivity were conducted as previously reported.[23−25] Krafft Temperature was determined visually using a 0.5 wt % suspension (Grant LTD 6G thermostat within ±0.1 °C). UV−vis absorption spectra were measured on a Unicam UV2 in 1 cm path length cells. All samples were diluted before with a few drops of ethanol (to destroy aggregates and get sharper spectra) and the appropriate amount of water. ^{1}H nuclear magnetic resonance (NMR) experiments were conducted in a JEOL Delta GX/270; samples were initially made up in D_2O and irradiated (or not), and the solvent was removed and replaced by acetonitrile-d_3 (Cambridge Isotope Laboratories, 99.8%). Liquid chromatography−mass spectroscopy (LC−MS) experiments were carried out in a Waters system (2700 sample

(23) Eastoe, J.; Paul, A.; Rankin, A.; Wat, R. *Langmuir* **2001**, *17*, 7873.
(24) Downer, A.; Eastoe, J.; Pitt, A.; Penfold, J.; Heenan, R. K. *Colloids Surf. A* **1999**, *156*, 33.
(25) Summers, M.; Eastoe, J.; Davis, S.; Du, Z.; Richardson, R.; Heenan, R. K.; Steytler, D. C.; Grillo, I. *Langmuir* **2001**, *17*, 5388.

manager; 600 Controller and 996 Photodiode Array Detector; column Phenomenex Luna 10u C8 reversed phase). An acetonitrile/water mobile phase gradient was used. MassLinx software was used to analyze the data (UV and mass spectra).

SANS. SANS experiments were carried out on the time-of-flight LOQ instrument at ISIS, U.K., as previously reported (e.g., ref 25) but using a 12 mm diameter beam. Hydrocarbon surfactant micelles were contrasted against D_2O, so that for a given shape the scattering intensity reports on particle number density (concentration). Absolute intensities were obtained by calibration with a partially deuterated polymer standard (described in ref 25). Measurements were conducted at 50 °C in circular quartz cells, 5 mm width and 1.8 cm diameter. The Q range was 0.02 → 0.25 $Å^{-1}$. To follow changes in aggregation after irradiation, a nonirradiated 10 mM (and 5 mM) sample in D_2O (Fluorochem, 99.9%) was measured. This was then irradiated for successive 5 s intervals (100 W Hg lamp), and SANS was run immediately. The illumination was gradually increased until a stationary state was achieved (125 s), and further irradiation (up to 815 s) did not affect the SANS pattern. Scattering data were fitted using the interactive FISH program,[26] a flexible multimodel suite that uses a standard iterative least-squares method for a variety of different form factors $P(Q)$, structure factors $S(Q)$, and polydispersity functions. Full accounts of these scattering laws are given elsewhere.[26−33] As described in Appendix 2, the model employed here was an equilibrium distribution of large unilamellar vesicles, polydisperse in radius and small charged micelles; the balance of populations (vesicle-to-micelle transition) depends on duration of irradiation.

Drop Shape Analysis and Contact Angle Measurements. Drop shape analysis and contact angle measurements were carried out in a Krüss DSA10 Drop Shape Analysis System, provided with a video framegrabber board (Falcon) and Krüss DSA1 software for control and data analysis. A purpose-made black box was used to eliminate background light and to reduce air-born vibrations. Samples were measured at room temperature (22 ± 2 °C). The substrates for contact angle studies were glass slides coated with OTS (Aldrich, 90+%), prepared as described previously.[34] A full account of the underlying theory can be found elsewhere.[35]

Photoexperiments. Aqueous dispersions of SGP were irradiated in quartz vessels (5 mL) with a 100 W high-pressure Hg white source, at concentrations above the critical micelle concentration (CMC) (conductivity) and therefore involved photoreactions with aggregated species. As confirmed by LC-MS and UV spectroscopy, the photoproducts were the same in all cases, and the reactions were monitored by UV−vis. Fresh drops for surface tension or contact angle measurements in the Krüss DSA were irradiated in situ for 1 min, and then, the tension or angle measurement was taken, and further irradiation did not change the outcomes. Because of small sample volumes, only short irradiation times were needed. For the reversibility experiments, diluted samples (10^{-5} M) were illuminated with monochromatic light. Initially, E-SGP was irradiated at 366 nm and then the photoproduct(s) were irradiated at 254 nm; changes were followed by UV−vis spectroscopy.

Computer Simulations. CAChe 3.2 (Oxford Molecular Ltd.) software was used to perform optimized geometry calculations using augmented MM3 parameters. UV−vis electronic transitions were generated by a ZINDO configuration interaction algorithm.

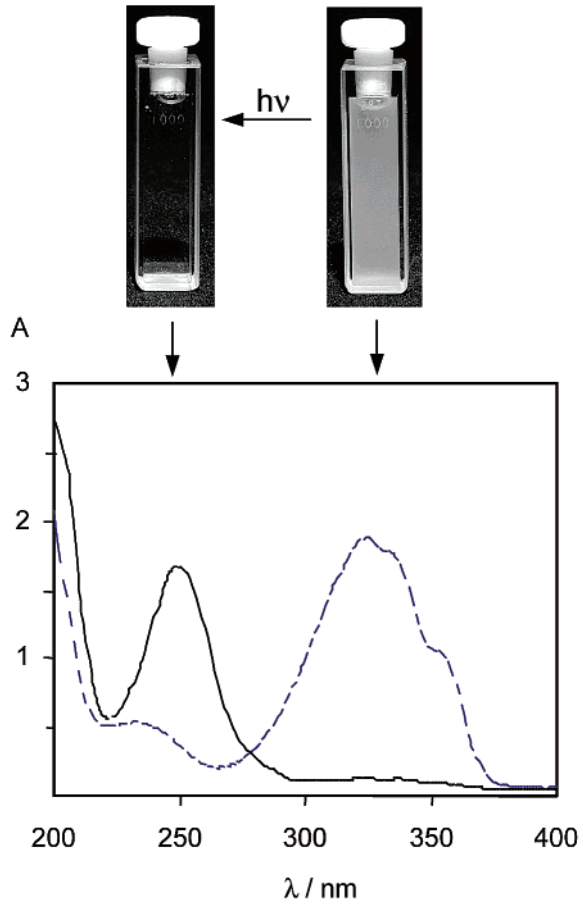

Figure 2. UV−vis absorption spectra of SGP surfactant (0.05 mM) and photographs of samples: (− − −) before irradiation, E-SGP, and (—) after irradiation, di-SGP.

Results and Discussion

(a) Solubility. E-SGP displayed a low solubility (water) at room temperature and the Krafft temperature, T_K, was found to be 50 °C. Associated T_K values were not determined for the photoproduct(s). However, after they were irradiated, the samples became transparent, even at room temperature, and remained clear (see inset to Figure 2). Therefore, the photoproducts probably aggregate differently than the starting E-SGP.

(b) Photochemistry. With such stilbenoid compounds, there are two dominant UV-induced reactions:[36,37] *cis*−*trans* isomerization and dimerization (Figure 1). Cyclization to phenanthrene derivatives is also possible, but this would require previous formation of the Z isomer. The photoreactions of aqueous dispersions of E-SGP, as well as solutions in acetonitrile-d_3 (CD_3CN), have been studied; this latter solvent was used in order to distinguish between a possible SGP dimer (di-SGP) and the Z-SGP isomer. Figure 2 shows absorption spectra obtained before and after irradiation (D_2O). The initial concentration of E-SGP was 10 mM (i.e., in the aggregated state), and both irradiated and nonirradiated samples were then diluted to an effective concentration of 0.05 mM to record the spectra. ^1H NMR spectra, seen in Figure 3, show clearly that in D_2O dimerization predominates over isomerization. The starting *trans E* isomer displays a peak at 7.4 ppm (Figure 3a), characteristic of the CH═CH group (between the aromatic rings); the signal at around δ 4.7, which predominates after irradiation in D_2O (Figure 3b), cor-

(26) Heenan, R. K. *FISH Data Analysis Program*; Rutherford Appleton Laboratory; Report RAL-89-129; CCLRC: Didcot, U.K., 1989.
(27) Hayter, J. B.; Penfold, J. *J. Chem. Soc., Faraday Trans. 1* **1981**, *77*, 1851.
(28) Kotlarchyk, M.; Chen, S.-H.; Huang, J. S.; Kim, M. W. *Phys. Rev. A* **1984**, *29*, 2054.
(29) Hayter, B. J. *Mol. Phys.* **1981**, *42*, 109.
(30) Hayter, B. J. *Mol. Phys.* **1982**, *46*, 651.
(31) Hayter, J. B.; Penfold, J. *Colloid Polym. Sci.* **1983**, *261*, 1022.
(32) Livesey, I. *J. Chem. Soc., Faraday Trans. 2* **1987**, *83*, 1445.
(33) Eastoe, J. *New Physico-Chemical Techniques for the Characterisation of Complex Food Systems*; Dickenson, E., Ed.; Blackie: Glasgow, 1995; p 268.
(34) Flinn, D. H.; Guzonas, D. A.; Yoon, R. H. *Colloids Surf. A* **1994**, *87*, 163.
(35) Rusanov, A. I.; Prokhorov, V. A. *Interfacial Tensiometry*; Elsevier Ed.: Amsterdam, 1996.
(36) Meier, H. *Angew. Chem., Int. Ed. Engl.* **1992**, *31*, 1399.
(37) Green, B. S.; Heller, L. *J. Org. Chem.* **1974**, *39*, 196.

Table 1. Characterization of Photoproducts: LC-MS and Computer Simulation Results

sample	simulated λ_{max} (nm)	LC-MS λ_{max} (nm)	LC-MS mass spec data *m/z*
E-SGP	327	325	388.5 [100, (M^{2+}/2)]
di-SGP (from D_2O experiment)	249	250	388.5 [100, (M^{4+}/4)]
Z-SGP (from acetonitrile-d_3 experiment)	245	245	388.5 [100, (M^{2+}/2)]

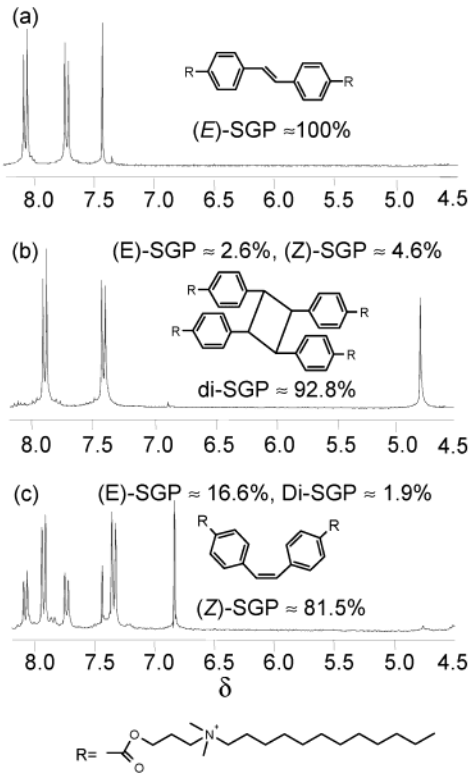

Figure 3. Partial ^{1}H NMR spectra of SGP surfactant: (a) before irradiation in CD_3CN, *E*-SGP; (b) after UV irradiation in D_2O, mostly di-SGP; and (c) after UV irradiation in CD_3CN, mostly *Z*-SGP.

responds to the protons in the cyclobutane region of a *cis*, *anti*, *cis* dimer,[37] whereas the peak around δ 6.8, which is the major component after irradiation in CD_3CN (Figure 3c), indicates the CH═CH group of the *cis Z* isomer.[9] LC−MS results and computer simulations presented in Table 1 support the assigned structures. In water, the calculated and measured absorbance maxima are consistent with the initial *E* form (325 nm), which is converted to the dimer (250 nm). The experiments in CD_3CN confirm that λ_{max} for the *Z* form is distinct from that of the dimer, supporting the conclusion drawn from chemical shift NMR patterns above. The values M^{n+}/n reported in Table 1 correspond to parent ions with relative molecular mass 777 for the *E* and *Z* forms but 1554 for the photoproduct obtained in water, corresponding to a single surfactant dication (*E* and *Z*) and a dimerized surfactant tetracation (the dimerized gemini surfactant). As discussed below (SANS section), it was confirmed that *E*-SGP forms aggregates (D_2O), whether the dimerization occurs within the aggregate or during the dynamic processes of micelle formation/break up is difficult to establish. Nevertheless, it is evident that in the organic solvent acetonitrile-d_3, where no or little aggregation is expected, isomerization is favored over dimerization. Therefore, as discussed in refs 36−38, it would appear that the process of dimerization in solution is certainly aggregation-dependent. On the other hand, whereas for

(38) Trecker, D. J. *Org. Photochem.* **1969**, *2*, 63.

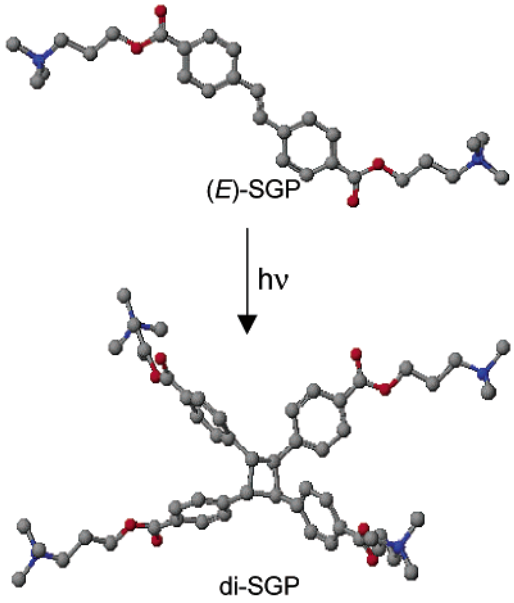

Figure 4. Changes in geometry of SGP surfactant spacer from a flat (*E*-SGP) to a nonflat structure (di-SGP) after irradiation. The hydrophobic chains are not shown.

a *trans* isomer the spacer should be mostly flat, the dimer possesses sp^3 carbons in the cyclobutane region; therefore, a twisted conformation is formed. Optimized geometry simulations (for the spacers only) support this view (Figure 4). Therefore, a change in aggregation may be expected because of the photochemical response.

Reversibility of the photoreaction was also studied using monochromatic light but with diluted samples (10^{-5} M owing to high extinction coefficient). In agreement with the above studies, irradiation of *E*-SGP at 366 nm produced a new band at 250 nm, indicative of the dimer. At 366 nm, absorption of the dimer is negligible; therefore, conversion to *trans* does not occur at this wavelength. Irradiation of this solution at 254 nm brings about the regeneration of the *trans* isomer, and a photostationary mixture of about 1:1 of dimer and *trans* form is reached. The spectra exhibit a clear isosbestic point at 278 nm, as indicated by the equilibrium spectra of Figure 2. It is clear that both species absorb at 254 nm, with the extinction coefficient of the dimer being ca. 5× that of the *trans* at this wavelength. Therefore, reversibility of the photoreaction is possible, at least in diluted systems. The back reaction might be improved by selecting a wavelength in which the *trans* form absorbs little, for example, around 262 nm.

(c) CMC and Surface Activity. CMC of the di-SGP was determined to be 0.3 mM by electrical conductivity. For experimental convenience, this was done at 25 °C, since the dimer gave stable transparent solutions at this temperature. With *E*-SGP, an approximate value of 0.19 mM was observed but this should be treated with caution since the solution was milky. A change from 25 to 50 °C is expected to increase CMC by a factor of 2−3,[39] and so, appropriate concentrations were studied. The results are

(39) Van Os, N. M.; Haak, J. R.; Rupert, L. A. M. *Physico-Chemical Properties of Selected Anionic, Cationic and Nonionic Surfactants*; Elsevier Ed.: Amsterdam, 1993; p 111.

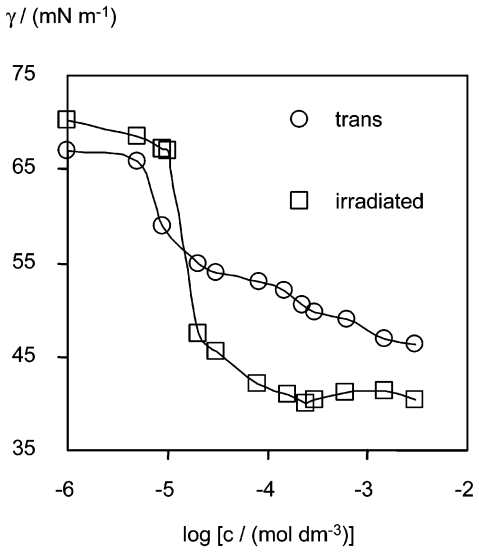

Figure 5. Equilibrium air−water surface tension γ_{eq} vs log conc for SGP surfactant at 50 °C in water: (○) before irradiation, *E*-SGP, and (□) after irradiation, di-SGP.

shown in Figure 5: in general, there is a decrease of around 8−6 mN m^{-1}, with a maximum change $\Delta\gamma \approx 10$ mN m^{-1} at 0.24 mM (for *E*-SGP = 50.5 and 39.9 mN m^{-1} for di-SGP). Note that with DVT slow tension decays can be followed (up to 10 min), and so, dynamic effects can be monitored. The data in Figure 5 represent "equilibrium" tensions, which were always achieved before 400 s for di-SGP and 150 s for *E*-SGP. Because of the establishment of a photostationary state (Figure 3), there is naturally a surfactant mixture (di-SGP, *E*-SGP, and *Z*-SGP), and this is expected to cause a "blurring" of the classic γ-ln c curve. It is probably also the reason for the minimum in the γ -ln c curve of di-SGP, which is normally attributed to an impurity, but this behavior is also seen in mixtures. For these reasons, it is inappropriate to analyze the tension isotherms in terms of the Gibbs adsorption equation. Furthermore, a clear CMC break point cannot be determined, although for irradiated di-SGP the minimum around 0.23 mM (≈ -3.5 on the log scale) is not inconsistent with the conductivity result. To clearly demonstrate photoactivity, drop shape analysis tension experiments were performed on 0.24, 1, and 3 mM solutions of *E*-SGP; examples of drops for the latter concentration are shown in Figure 6a,b. For all three concentrations, $\Delta\gamma$ was similar, around 10 ± 2 mN m^{-1} lower after irradiation, which is clearly evident since the drops become more elongated. Contact angle measurements on OTS-coated slides (literature values $\theta_{water} = 102-110°$[34]) were also performed, and example results are shown in Figure 6c,d for drops 25 min after deposition. The decrease in θ was also followed as a function of time, up to 25 min, and a constant $\Delta\theta$ ($\theta_{di-SGP} - \theta_{E-SGP}$), around −15°, was always seen irrespective of the drop age. Furthermore, the final values of $\theta_{di-SGP} = 52.5°$ and $\theta_{E-SGP} = 67.5°$ showed the same decrease. This improvement in wetting properties amplifies the surface tension results; in all cases, surface activity was enhanced after irradiation.

Generally speaking, an improvement in surface activity is found comparing a gemini surfactant with its "monomeric" counterpart.[40] One explanation[40] relies on a distortion of water structure by the hydrophobic groups; with a gemini, the perturbation is more pronounced. Another idea[40] is based on interfacial packing, since the area-per-chain of a series of bisquaternary ammonium salts is lower than for the corresponding monomeric surfactant. Considering the present system, *E*-SGP was comprised of two tails (and headgroups), whereas there are four in di-SGP; this could magnify interfacial packing and reduce tensions. Added to this is the transition from a mostly rigid to a "semiflexible" spacer (which might offer more possibilities for enhanced interfacial packing).

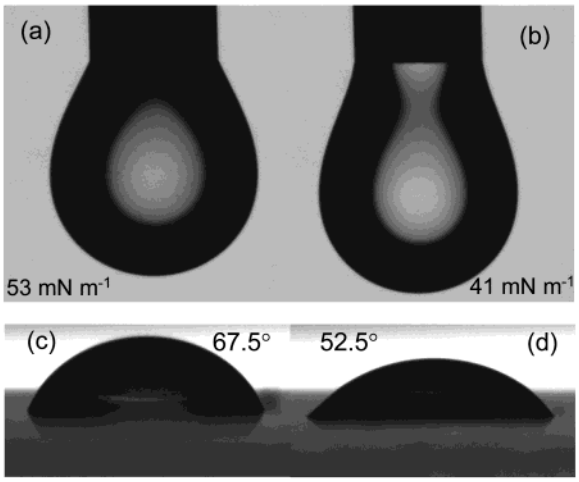

Figure 6. Samples of aqueous SGP. Pendant drops 1.0 mM: nonirradiated and irradiated samples a and b, respectively. Sessile drops 0.24 mM of nonirradiated and irradiated samples c and d, showing changes in contact angle.

(d) SANS. SANS was used to follow changes in aggregation caused by successive 5 s bursts of white UV. These kinetic runs showed a gradual (and reproducible) conversion from one state to another, and Figure 7a displays example curves measured between 0 and 125 s irradiation times. Initially, the surfactant is present as *E*-SGP, and finally, there is a mixture in which di-SGP dominates. A significant change in the $I(Q)$ profile is evident, and this goes hand-in-hand with the visual appearance of the system (photoinset to Figure 2).

At low Q, the initial state displays a clear Q^{-2} scattering (readily seen on the log−log scale). Although this power law can be interpreted in various ways (e.g., Gaussian coils or vesicles), none of which can be completely ruled out, a polydisperse core−shell vesicle form factor is clearly consistent with the scattering (see Appendix 2 for details). The milky appearance of the initial *E*-SGP solution (Figure 2 inset) may be due to the presence of a lamellar dispersion, and so, the use of a vesicle form factor does have some basis. Evidently, this scattering law works well, although it represents one of a number of possibilities, all of which correspond to large extended aggregation structures (note the apparent absence of $S(Q)$ could be due to a combination of the restricted Q range and an effectively low concentration of the large aggregates). The fitted lines represent a thickness of 20 Å (fixed), and Figure 7b gives example vesicle size distributions. This apparent bilayer thickness is small as compared with the molecular size (C12 chain length ~ 17 Å) and may be down to highly efficient packing, or stacking, of individual molecules within the aggregate; only detailed contrast variation experiments can answer this question.

On the other hand, the final state exhibits a clear peak maximum centered on $Q \sim 0.05$ Å^{-1}, which is a signature of charged micelles.[27,29−31] As shown by the fits in Figure 7a, the combined vesicle−ionic spherical micelle scattering

(40) Menger, F. M.; Keiper, J. S. *Angew. Chem., Int. Ed.* **2000**, *39*, 1906.

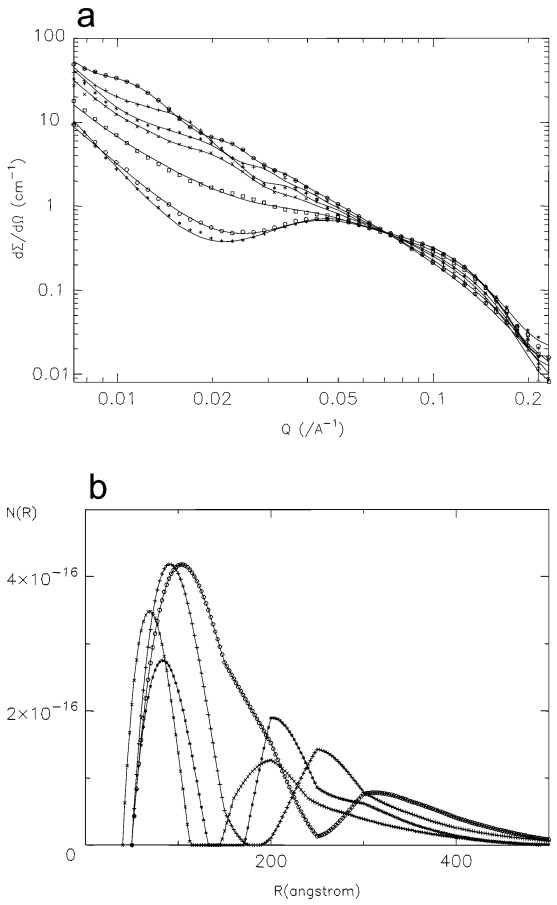

Figure 7. (a) SANS data for a 10 mM aqueous solution of SGP surfactant as a function of irradiation time. In order of decreasing intensity 0 (⊙), 10 (+), 20 (*), 30 (×), 55 (□), 95 (○), and 125 s (★) irradiation time. The fitted lines are for polydisperse vesicles (bilayer thickness = 20 Å) in equilibrium with charged micelles (radius = 20 Å, fractional molecular charge + 0.25 and variable Debye length between 100 and 35 Å). (b) Example vesicle size distributions for the 0, 10, 20, and 30 s data from part a, using the same symbols.

Table 2. Distribution of Aggregate Types as a Function of Irradiation Time, Based on Analysis of SANS Data[a]

t/s	% vesicle	% sphere	t/s	% vesicle	% sphere
0	98.5	1.5	30	46.5	53.5
10	87.0	13.0	55	34.3	65.7
20	60.3	39.7			

[a] Vesicle shell thickness = 20 Å; small sphere radius = 20 Å; spherical micelle charge = 20; and variable Debye length (between 100 and 35 Å).

law represents the data well, with radius 20 Å, fractional charge +0.25 per molecule, and a Debye length of 35 Å for the longer irradiation times. Furthermore, this mixed model fitted the absolute intensities better than other scattering laws that were tested (Appendix 2). This radius value is more realistic for disordered C12 chain surfactants and compares favorably with the classic example of SDS (~25 Å). On the basis of this model, it appears that the vesicles become smaller, with a sharper size distribution, and this is consistent with a shift from large aggregates to small micelles. From absolute scattering intensities, it is possible to estimate how the proportion of aggregates shifts from vesicles to micelles (Table 2). At the longer times of 95 and 125 s (and also after 815 s, data not shown but the same as 125 s), the majority of scattering arises from the charged micelles, although there is a small population of residual vesicles (~10−20%). Irrespective of the interpretation, it is clear that UV induces dramatic changes in aggregation (Figures 2, inset, and 7). Although dynamic information is, in principle, available from these data, the interpretation will be to some extent form factor-dependent, and so, a detailed kinetic interpretation is inappropriate at this stage.

Summary and Conclusions

A new SGP has been synthesized and purified, and its physicochemical properties have been investigated. The rationale for this work was to design an optimized photoactive surfactant that displays enhanced sensitivity, good chemical stability, and clean photoreactions. Employing a photoactive chromophore in the headgroup spacer results in large changes in the relative orientation of hydrophobic chains, which feeds through to significant effects in the interfacial and aggregation properties.

As shown in Figures 1 and 2 and Table 1, a range of spectroscopic and chromatographic methods (UV−vis, ^{1}H NMR, and LC−MS) indicate that photodimerization is preferred over *trans*−*cis* isomerization, at least in aqueous solutions. Partial reversibility has been demonstrated in very dilute aqueous solutions. On the other hand, in an organic solvent acetonitrile, isomerization appears to be the dominant pathway. UV irradiation caused macroscopic and microscopic changes that are consistent with a break up of polydisperse large vesicle-like aggregates to form small spheroidal charged micelles (Figures 2, inset, and 7). Interfacial properties are also strongly affected; maximum changes are a 10−12 mN m^{-1} reduction in air−water surface tension (Figures 5 and 6) and a 15° in contact angle at a hydrophobic surface (Figure 6). Taken together, the results show that sophisticated molecular designs are key to unlocking the potential of photosurfactants. It is hoped that the findings stimulate further research into this intriguing system, which has many potential applications for control over solubilization, delivery systems, rheology, surface and interfacial tension, and wetting.

Acknowledgment. M.S.-D. is grateful to the Mexican organization CONACyT (National Council of Science and Technology, Grant No. 151737) for a scholarship. We also acknowledge CLRC for allocation of beam time at ISIS and grants toward consumables and travel. Special thanks to Drs. Russell Cox, Martin Murray, and Prof. Roger Alder for their valuable advice in LC−MS, ^{1}H NMR, and computer simulation studies, respectively.

Appendix 1: Synthesis of the Photosurfactant

Where appropriate, a dry nitrogen atmosphere was employed following standard techniques. In the subsequent procedures, petrol refers to petroleum ether (boiling range 40−60 °C). Thin-layer chromatography (TLC) was used to monitor the reactions (silica gel plate, 19:1 petrol:ethyl acetate or 2:1 dichloromethane:petrol). All intermediates and the final product were dried at 40 °C, 1 mm Hg for at least 48 h. ^{1}H NMR (JEOL Delta GX/270), elemental analysis, and mass spectrometry (VG Analytical Autospec, low resolution or LC−MS, Waters System) were used to characterize intermediates and products. The results were in agreement with the expected chemical structures.

4-Bromomethyl Methylbenzoate (1). A modified literature procedure[41] was employed. Methyl *p*-toluate (11.4 g, 75.0 mmol; Acros, 99%), *N*-bromosuccinimide (14.8 g, 78.0 mmol; Avocado, 99%), and azobis(cyclohexanecar-

(41) Steenwinkel, P.; James, S.; Grove, D.; Veldman, N.; Spek, A.; Van Koten, G. *Chem. Eur. J.* **1996**, *2*, 1440.

bonitrile) (0.35 g; Aldrich, 98%) were heated to reflux in anhydrous methyl formate (85 mL; Aldrich 99%) under illumination (200 W incandescent bulb) for 42.5 h. The solvent was removed under reduced pressure, and the residue was dispersed in ether and brought to reflux. After the insoluble material was removed by filtrating and concentrating, the solid was precipitated from ether with hexane. The remaining succinimide was extracted with water, and the solid was dried to give white crystals of 4-bromomethyl methylbenzoate (8.06 g, 54%); mp 52 °C (literature[42] 50−53 °C). δ_H ($CDCl_3$): 3.94 (3H, s, CO_2CH_3), 4.52 (2H, s, $ArCH_2Br$), 7.46 (2H, d, $J = 8.1$ Hz, *meta*-Ar*H*), 8.01 (2H, d, $J = 10.8$ Hz, *ortho*-Ar*H*).

4-Carbomethoxybenzyl(Triphenyl)phosphonium Bromide (2). A modified literature procedure[43] was employed. 4-Bromomethyl methylbenzoate (7.76 g, 35.0 mmol) and triphenyl-phosphine (12.0 g, 45.5 mmol; Aldrich, 99%) were stirred in toluene (96 mL; Anala R, 99.5%) for 48 h at room temperature. The solvent was removed under reduced pressure, and the solid was repeatedly washed with petrol. The collected product was dried to give 4-carbomethoxybenzyl(triphenyl) phosphonium bromide as a white powder (16.6 g, 97.0%); mp 232 °C. δ_H (CD_2Cl_2): 3.88 (3H, s, CO_2CH_3), 5.51 [2H, d, $ArCH_2P(C_6H_5)_3$], 7.22 (2H, d, *meta*-Ar*H*), 7.76 (17H, m: 15H $P(C_6H_5)_3$ and 2H *ortho*-Ar*H*).

***E*-4,4′-Dicarbomethoxystilbene (3).** 4-Carbomethoxybenzyl(triphenyl) phosphonium bromide (14.4 g, 29.0 mmol) was stirred with anhydrous methanol (78 mL). Sodium methoxide solution was prepared by mixing sodium (1.56 g, 68 mmol: BDH) and anhydrous methanol (39 mL; Aldrich, 99.8%). This was added to the reaction flask to give a yellow solution, which was warmed to 40−45 °C for 40 min. After it was cooled (ice), the mixture was treated dropwise with 4-formyl methylbenzoate (3.90 g, 26.0 mmol; Acros, 99%) in anhydrous methanol (52 mL). After it was completely added, the mixture was heated to reflux for 1 h and then cooled (ice) and concentrated hydrochloric acid (7.8 mL) was added. The reaction mixture was filtered; the mother liquor was evaporated to dryness. The product was extracted from the solid by toluene, then ethyl acetate, and then chloroform. Solvents were removed under reduced pressure, and the crude product was dissolved in boiling heptane, followed by addition of a few crystals of iodine. After it was exposed to sunlight (7 days minimum), crystals formed, which were recrystallized from tetrahydrofuran (THF) and petrol. The product was dried to yield white crystals of *trans*-4,4′-dicarbomethoxystilbene (3.51 g, 41.0%); mp 247 °C (literature[44] 236−238 °C). δ_H (CD_2Cl_2): 3.91 (3H, s, CO_2CH_3), 7.28 (2H, s, Ar*CH*=*CH*Ar), 7.64 (4H, d, 2 × *meta*-Ar*H*), 8.04 (4H, d, 2 × *ortho*-Ar*H*).

***E*-Stilbene-4,4′-dicarboxylic Acid.** The method of Hager, Vanarendonk, and Shonle was followed.[45] Yield: 2.90 g, 91%; mp > 320 °C (literature[46] > 320 °C, literature[47] 460 °C, sealed tube). δ_H (dimethyl-d_6 sulfoxide): 7.49 (2H, s, Ar*CH*=*CH*Ar), 7.76 (4H, d, 2 × *meta*-Ar*H*), 7.96 (4H, d, 2 × *ortho*-Ar*H*).

***E*-Stilbene-4,4′-dicarbonyl Dichloride.** A previously reported method was followed.[46] Yield: 1.87 g, 68%; mp 207 °C (literature[46] 222−228 °C). δ_H (dimethyl-d_6 sulfoxide): 7.49 (2H, s, Ar*CH*=*CH*Ar), 7.76 (4H, d, 2 × *meta*-Ar*H*), 7.95 (4H, d, 2 × *ortho*-Ar*H*).

***E*-Bis(3-bromopropyl)-4,4′-stilbenedicarboxylate.** *E*-Stilbene-4,4′-dicarbonyl dichloride (1.83 g, 5.44 mmol) and 3-bromopropanol (25.0 g, 17.5 mol; Aldrich, 97%) were stirred at 45 °C for 14 h. The mixture was dissolved in dichloromethane, washed with water twice, and then dried overnight with magnesium sulfate. After solvent was removed, a white gum was recovered and a solid was precipitated after addition of diethyl ether. Purification was done by flash column chromatography using silica gel and eluting with dichloromethane:petrol 2:1 and graduating to 10:1 dichloromethane:petrol. The product was dried to yield white crystals (2.20 g, 72.0%); mp 108−110 °C. δ_H (CD_2Cl_2): 2.25 (4H, m, 2 × $OCH_2CH_2CH_2Br$), 3.51 (4H, t, 2 × $OCH_2CH_2CH_2Br$), 4.37 (4H, t, 2 × $OCH_2CH_2CH_2Br$), 7.21 (2H, s, Ar*CH*=*CH*Ar), 7.55 (4H, d, 2 × *meta*-Ar*H*), 7.95 (4H, d, 2 × *ortho*-Ar*H*).

***E*-SGP.** *E*-Bis(3-bromopropyl)-4,4′-stilbene-dicarboxylate (1.00 g, 1.96 mmol) and *N*,*N*′-dimethyl-*N*-dodecylamine (1.2 mL, 4 mmol; Aldrich, 97%) were stirred in dry toluene (30 mL) at 100 °C for 40 h. The solvent was removed under reduced pressure. The crude product, a yellowish gum, was stirred at room temperature in acetone for 2 h and then filtered and washed with acetone. At this stage, white powder was obtained (1.13 g, 62%). A final purification was done (to eliminate dust particles) by dissolving the product in acetonitrile, followed by filtration (glass sinter). The solvent from the filtered liquor was removed under reduced pressure. The product was dried to yield white crystals (1.01 g, 55.4%); mp 206−207 °C. δ_H (acetonitrile-d_3): 0.86 (6H, t, 2 × CH_2CH_3), 1.27 (36H, m, 2 × $(CH_2)_9$), 1.7 (4H, broad, 2 × $N(CH_3)_2CH_2CH_2$), 2.2 (4H, broad, 2 × $OCH_2CH_2CH_2N$), 3.05 (12H, s, 2 × $N(CH_3)_2$), 3.27 [4H, t, 2 × $N(CH_3)_2CH_2$], 3.48 (4H, t, 2 × $OCH_2CH_2CH_2N$), 4.38 (4H, t, 2 × $OCH_2CH_2CH_2$), 7.43 (2H, s, Ar*CH*=*CH*Ar), 7.73 (4H, d, 2 × *meta*-Ar*H*), 8.07 (4H, d, 2 × *ortho*-Ar*H*). Electrospray: *m*/*z* 388.5 ([M^{2+}]/2, 100%). FAB: *m*/*z* 762 ([$M^{2+} - CH_3$], 100%).

Appendix 2: SANS Theory

The SANS scattering cross-section for a reasonably dilute system of N_p particles is given by the product of a form, or shape, factor $P(Q)$ and an interparticle structure factor $S(Q)$.

$$[d\sum(Q)]/[d\Omega] = N_p P(Q) S(Q) \qquad (1)$$

For a dilute, noninteracting system, $S(Q)$ tends to unity and may be ignored, else wise it may be calculated for hard spheres in the Percus−Yevick approximation or for charged spheres in the RMSA approximation.[27] Here, $S(Q)$ was also corrected for the effects of polydispersity using the method of Chen et al.[28] For a polydisperse system of particles, the form factor is simply summed over a size distribution $N(R)$.

$$P(Q) = (\rho_p - \rho_m)^2 \int N(R) F^2(Q,R)\, dR \qquad (2)$$

For a sphere of radius R, $F(Q,R) = f(Q,R)$ and is given by

$$f(Q,R) = V(R)\frac{3(\sin(QR) - QR\cos(QR))}{(QR)^3} \qquad (3)$$

where $V(R) = (4\pi/3)R^3$. For a hollow spherical shell of

(42) Pernía, G. J.; Kilburn, J. D.; Essex, J. W.; Mortishire-Smith, R. J.; Rowley, M. *J. Am. Chem. Soc.* **1996**, *118*, 10220.
(43) Terfort, A.; Brunner, H. *J. Chem. Soc., Perkin Trans. 1* **1996**, *2*, 1467.
(44) Russell, G. A.; Becker, H. D. *J. Am. Chem. Soc.* **1963**, *85*, 3406.
(45) Hager, G.; Vanarendonk, A.; Shonle, H. *J. Am. Chem. Soc.* **1944**, *66*, 1982.
(46) Khalaf, A. I.; Pitt, A. R.; Scobie, M.; Suckling, C. J.; Urwin, J.; Waigh, R. D.; Fishleigh, R. V.; Young, S. C.; Wyllie, W. A. *Tetrahedron* **2000**, *56*, 5225.
(47) Toland, W. G.; Wilkes, J. B.; Brutschy, F. J. *J. Am. Chem. Soc.* **1953**, *75*, 2263.

inner radius r and thickness Δ

$$F(Q,r) = f(Q,r) - f(Q,r + \Delta) \quad (4)$$

In either case, the total volume of the dispersed particle may be simply computed given absolute scattered intensities and the neutron scattering length densities of the particle ρ_p and solvent medium ρ_m. For a large radius, rigid, hollow sphere, or vesicle, the form factor $P(Q)$ has a characteristic oscillation caused by interference between scattering from opposite faces of the sphere. While a Schultz distribution[28] for $N(R)$ (similar to a log-normal) adequately described the SANS signal, at middle and high Q, it appeared that certain vesicle radii were more common than others. An essentially bimodal distribution of vesicle radii provided a significantly better fit to the oscillations at small Q. The "free form" distribution $N(R)$ covered the range $r = 50$ to about 500 Å with 10 adjustable height "sticks", the distribution $N(R)$ being made smooth and continuous by a local cubic interpolation between an adjacent group of four sticks (any negative values set at zero). The value of $N(R)$ at the first and last sticks was also kept at zero, leaving essentially eight adjustable parameters, though as the reaction proceeded and the vesicles became smaller, the sticks were grouped more toward smaller radii.

Prior to irradiation, the Q^{-2} scattering was consistent with vesicles (sheets) (e.g., refs 26 and 33). SANS from the postirradiated samples could be interpreted as a mixed population of polydisperse vesicles and much smaller charged micelles as described by the Hayter−Penfold model.[27,29−31] Because of the large number of (possible) free parameters, some of these were input as constants, based in initial trial fits: vesicle layer thickness, 20 Å; micelle radius, 20 Å; and fractional molecular charge, +0.25. The distribution in vesicle radius $N(R)$ and Debye length (100−35 Å) were allowed to vary, as was the fraction of aggregates present as vesicles (Table 1). To check the validity of the model, a calculated scale factor was compared to a theoretical value based on the known composition. The possibility of ellipsoidal micelles was also tested by use of the appropriate form factor. However, because of the many contributions to the scattering, it was difficult to clearly distinguish between mildly ellipsoidal particles (aspect ratio 1.3−1.5) and spherical particles.

LA0257384